Substantial enhancement of thermal spin polarization in Py/Cu interface

Shaojie Hu,[1,2] Jingyan Zhao,[3] Lei Wang,[1] Xiaomin Cui,[4] Kohei Ohnishi,[2,5] Taisei Ariki,[5] Tai Min,[1] Ke Xia,[6,*] and Takashi Kimura[2,5,†]

[1]*Center for Spintronics and Quantum Systems, State Key Laboratory for Mechanical Behavior of Materials, Xi'an Jiaotong University, Xi'an, Shaanxi 710049, China*

[2]*Research Center for Quantum Nano-Spin Sciences, Kyushu University, 744 Motooka, Fukuoka 812-8581, Japan*

[3]*The Center for Advanced Quantum Studies and Department of Physics, Beijing Normal University, Beijing 100875, China*

[4]*Shaanxi Key Laboratory of Condensed Matter Structures and Properties, School of Science, Northwestern Polytechnical University, Xi'an 710072, China*

[5]*Department of Physics, Kyushu University, 744 Motooka, Fukuoka 812-8581, Japan*

[6]*Shenzhen Institute for Quantum Science and Engineering (SIQSE) Department of Physics, Southern University of Science and Technology (SUSTech), Xueyuan Avenue 1088, Nanshan District, Shenzhen, P. R. China*

(Received 5 March 2018; revised manuscript received 9 September 2018; published 9 October 2018)

We investigated the temperature dependence of thermally excited spin current properties of ferromagnet Py ($Ni_{80}Fe_{20}$) by using a lateral spin-valve structure. The spin-dependent Seebeck coefficient at the Py/Cu interface was found to show a significant increase at low temperature while the charge Seebeck coefficient showed the ordinal reduction with decreasing temperature. This produces a crossover between the charge- and spin-dependent Seebeck coefficients, resulting in the thermal spin polarization greater than 100% below 125 K. From the first-principles calculation specially developed for the Py/Cu interfaces, the spin-dependent Seebeck coefficient is found to be highly susceptible to the magnetic disorder-induced scattering at the interface. The calculation with considering the temperature dependence of the magnetic disorder provides a consistent description for the significant enhancement of spin-dependent Seebeck coefficient in the Py/Cu interface. Our demonstration shows the importance of interface disorder and paves the way toward the development of conventional ferromagnetic metal for the practical application of thermo-spin energy conversion.

DOI: 10.1103/PhysRevMaterials.2.104403

I. INTRODUCTION

The combination between the ferromagnet and other functional materials offers a variety of spin-conversion phenomena under the interplay between the spin-orbit and spin-exchange interactions. The discovery of the thermally excited spin current promoted the research on the conversion between the spin and heat and developed a new branch of spintronics, called spin caloritronics [1–4]. This emerging research provides new concepts for thermoelectric energy-harvesting devices in association with spin-dependent transport and spin transfer toque [5–15]. The spin Seebeck effect (SSE) is one of the representative spin caloritronic phenomena which was first demonstrated by detecting the inverse spin Hall effect in permalloy (Py)/Pt hybrid structures by Uchida *et al.* [2]. However, since the SSE in metallic systems are contaminated by various spurious effects such as anomalous Nernst effects [16–19], it is only effective in the bilayer system consisting of the magnetic insulator, where the SSE can be understood by thermally excited spin pumping [4].

Instead of SSE, the thermal spin injection, which is a relatively simple way for utilizing the heat in spintronic devices, is also recognized as the unique method for creating the spin current [1]. Here, the temperature gradient at the interface between ferromagnetic metal (FM) and nonmagnetic metal (NM) produces spin injection because of the difference in the spin-related Seebeck coefficient between the FM and NM. To realize efficient thermal spin injection, the difference in the Seebeck coefficient between up and down spins is the key factor. Since the Seebeck coefficient is determined by the energy derivative of the logarithmic density of state around the Fermi level [20], the thermal spin injection is expected to have the different characteristic from the electrical spin injection.

Note that the sign of the Seebeck coefficient can be either positive or negative whereas the sign of the electrical conductivity is always positive. If the signs of the Seebeck coefficient for the up-spin electron and that for the down-spin electron are opposite each other, the temperature gradient efficiently produces a spin current because of the opposite movement of the up-spin and down-spin electrons. Thus, the thermally excited spin current is expected to be an efficient method for manipulating the spin current.

The first experimental demonstration of thermal spin injection has been reported by Slachter *et al.* [3]. By manipulating the heat flow due to a Joule heating in a specially developed laterally configured FM/NM hybrid nanostructure, they succeeded in detecting the thermally excited spin-valve signal even at room temperature. The thermal spin injection in a magnetic tunnel junction was also demonstrated to

*xiak@sustc.edu.cn
†t-kimu@phys.kyushu-u.ac.jp

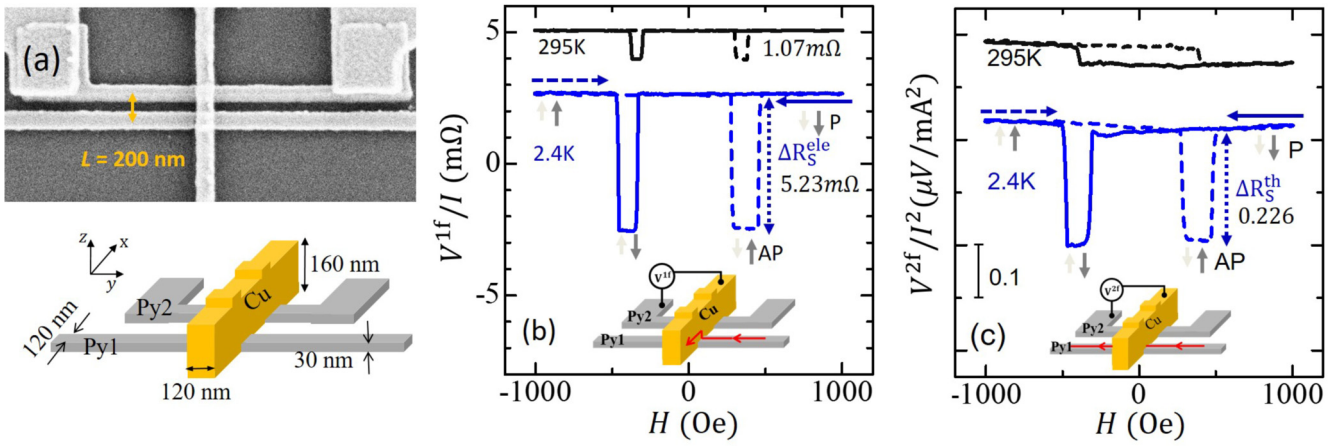

FIG. 1. (a) SEM image of the fabricated Py/Cu LSV together with a schematic illustration. Two Py electrodes are separated by 200 nm from center to center. (b) Electrically driven nonlocal spin signals for Py/Cu/Py LSV measured at 295 K (black curve) and 25 K (blue curve) together with the probe configuration. The electrical spin signal ΔR_S^{ele} is defined as the overall voltage change normalized by the bias current. The magnetization configurations at each state are shown by small arrows. The long solid and dotted arrows indicate the direction of the field sweep. (c) Thermally excited nonlocal spin-valve signals for the Py/Cu/Py LSV measured at 295 K (black curve) and 25 K (blue curve) together with the probe configuration. The thermal spin signal ΔR_S^{th} is defined as the overall change of the second-harmonic voltage normalized by the bias current squared.

produce large spin-dependent thermoelectric voltage owing to their interface resistances [21]. However, in these studies, the thermally excited spin currents were still inefficient compared with the electrically excited one. Very recently, we demonstrated that CoFeAl has an excellent thermal spin-injection property because of its favorable band structure [22,23]. A highly efficient thermal spin polarization greater than 100% was obtained because the Seebeck coefficient shows a different sign depending on the spin direction [24].

It is well known that the theoretical approaches such as *ab initio* calculations and density functionals are highly effective for seeking and/or designing an appropriate material. Since the spin-dependent Seebeck coefficient can be tuned by materializing the band structure, it may be possible in principle to design the material with the ideal band structure for the efficient thermal spin injection [25,26]. However, it is not so simple to reproduce realistic electrical and thermal transport properties from the band-structure calculation based on a first-principles study. This is because the calculation of the scattering matrix at a FM/NM interface and/or the surface needs the complicated quantum-mechanical treatments. In particular, the calculation including the interface disorders is very challenging and is an important milestone. Since the interface magnetism and the transport properties are expected to show strong temperature dependence [27], the temperature evaluation of the thermal spin-injection property may provide useful information for the quantitative investigation of the interface disorder. Indeed, in the case of the nonmagnetic heavy metal and magnetic insulator, the enhancement of interface coupling between magnon and phonon was obtained from the temperature dependence of the spin Seebeck effect [28–30]. Thus, understanding of the thermo-spin effect in metallic interfaces is indispensable for developing advanced spin caloritronic materials. However, according to our knowledge, the temperature dependence of the thermal-spin-injection property in the metallic systems has not been investigated intensively so far. From these viewpoints, in the present study, we investigate the temperature dependence of the thermal spin-injection property by using a lateral spin-valve structure.

II. EXPERIMENTAL METHOD

As a target interface, we adapt the Py/Cu interface, which is commonly used in the fundamental experiments for metallic spintronics. Although the thermal-spin-injection efficiency of the Py/Cu interface is known to be low at room temperature [31], a highly-spin-polarized CoFeAl electrode enables us to evaluate the spin accumulation precisely [22,23]. Here, we prepared two kinds of lateral spin valves. One is a Py/Cu/Py LSV and the other is Py/Cu/CoFeAl. Lateral spin valves (LSVs) were fabricated by multiple-step electron-beam lithography on a thermally oxidized Si substrate. Here, both Py and CoFeAl were deposited by electron-beam evaporation at a pressure of 1.1×10^{-9} torr. A Cu strip was deposited by Joule evaporation under a pressure of 1.1×10^{-8} torr. Here, the thicknesses for Py and CoFeAl are 30 nm and that for Cu is 160 nm. The electrical resistivities for CoFeAl, Py, and Cu are 45.0 $\mu\Omega$ cm, 29.0 $\mu\Omega$ cm, and 2.8 $\mu\Omega$ cm, respectively, at 295 K. The interfaces between the FM and Cu were carefully cleaned by low-voltage Ar-ion milling, assuring a clean interface. Figure 1(a) shows a scanning electron microscope image and schematic illustration of the fabricated Py/Cu/Py LSV. Here, one FM wire is connected to the large pad at the end while the other one has flat end shapes. This enables us to control the switching of magnetization configuration by adjusting the magnetic field. The center-center distance between two FM wires is 350 nm. The transport properties of the electrically and thermally excited spin currents have been evaluated by using standard lock-in detection techniques.

III. EXPERIMENTAL RESULTS AND DISCUSSION

First, we evaluate the electrically excited spin current injection and detection properties for Py/Cu/Py LSVs by

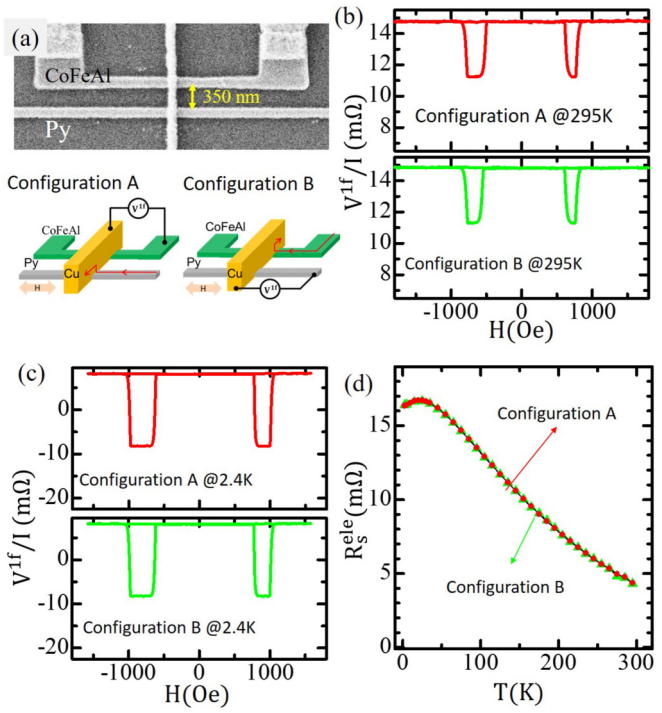

FIG. 2. (a) Schematic illustration of the two measurement configuration for the electrical spin injection. Electrical spin-valve signals measured for measurement Configuration A (red curve) and Configuration B (green curve) at (b) 295 K and (c) 25 K. (d) Temperature dependence of electrical spin signal ΔR_S^{ele} for two measurement configurations.

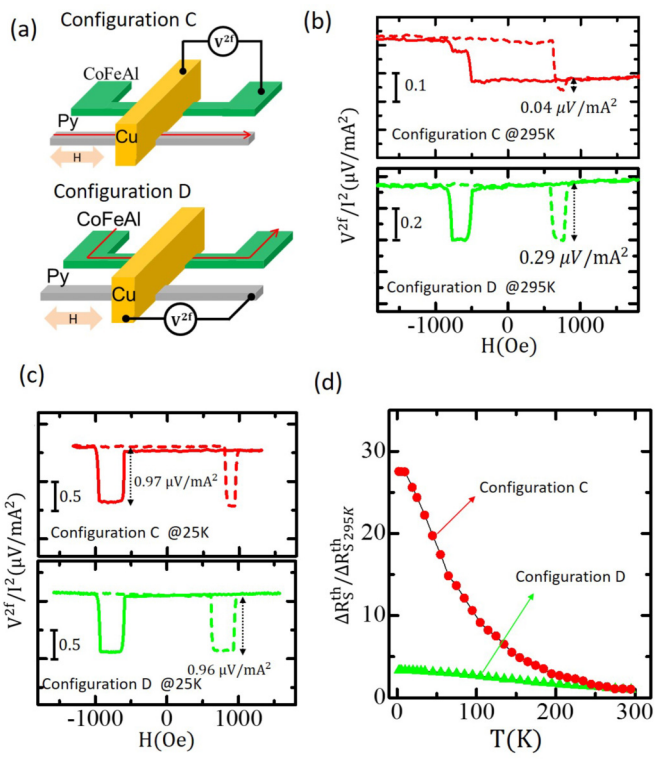

FIG. 3. (a) Schematic illustration of the two measurement configurations for the thermal spin injection. Thermally driven nonlocal spin-valve signals for measurement Configuration C (red curve) and Configuration D (green curve) measured at (b) 295 K and (c) 25 K. (d) Temperature dependence of the thermal spin signals for Configuration C and Configuration D. Here, the vertical axis is normalized by the value at 295 K.

measuring the nonlocal spin-valve signal. As can be seen in Fig. 1(b), we observed clear spin-valve signals both at 295 and 25 K. Here, the magnitude of the value change between the parallel and antiparallel states is known as the spin signal, which is the barometer for evaluating the performance of LSVs. The electrical spin signal is enhanced by a factor of 4.0 from 295 to 25 K. The main reason for the enhancement of the spin signal is the reduction of the spin-flip scattering due to phonons in the Cu. A small increase of the electrical spin polarization also contributes to this enhancement [32–34].

Next, we evaluate the thermal spin-injection property for the Py/Cu/Py LSV. The thermally excited spin signal was detected from the second-harmonic measurement with the probe configuration shown in the inset of Fig. 1(c). Figure 1(c) shows the nonlocal second-harmonic spin signal curves under thermal spin injection. Although a clear spin-valve signal is observed as 0.226 μV/mA^2 at 25 K, it is hard to see the spin-valve signature at 295 K. So, the spin-valve signal due to the thermal spin injection is smeared out by the asymmetric field dependence of the signal. This can be understood by invoking the anomalous Nernst effect of the ferromagnetic detector [35,36]. From the signal-to-noise ratio, we can say that the thermally excited spin signal at 295 K is less than 0.01 μV/mA^2. Here, we emphasize that thermal spin signal at 25 K is at least 20 times larger than that at 295 K. This factor is much larger than that for electrical spin injection. Thus, the remarkable increase of the thermal spin signal at low temperature implies that thermal spin injection is more sensitive to the interface disorder than is electrical spin injection. This is reasonable because the Seebeck coefficient is proportional to the energy derivative of the energy-dependent electrical conductivity.

To more precisely estimate the thermal-spin-injection efficiency at 295 K, we used a Py/Cu/CoFeAl LSV, where the highly-spin-polarized CoFeAl electrode enables us to detect the tiny thermal spin current. Figure 2 shows the characteristics for electrical spin injection. The obtained spin signal is three times larger than that in the Py/Cu/Py LSV because of the high spin polarization of CoFeAl. We can clearly confirm the reciprocal relationship of the electrical spin signal by interchanging the current and voltage probes [37]. This can be deduced from the analytical equation based on the one-dimensional spin-diffusion model [38]. As can be seen in Fig. 2(d), the spin signal increases with decreasing temperature above 25 K because of suppression of the phonon-mediated spin-flip scattering. The spin signal slightly reduces below 25 K. This is a common feature for the metallic LSVs and can be explained by surface scattering and other mechanisms [32,39]. The ratio of the spin signal at 295 K to that at 25 K is 3.8, which is also the typical value observed in the metallic LSVs with the short interval.

Figure 3 shows the thermally excited spin injection and detection properties of Py/Cu/CFA LSVs. Although the

asymmetric field dependence still remains at 295 K, a spin-valve signal with the magnitude of 0.04 μV/mA^2 is clearly confirmed for the measurement configuration C with the Py injector and CFA detector. From these results, we can precisely estimate the ratio of the thermal spin signal between 295 and 25 K as approximately 24.0 for the Py/Cu injector. This is much larger than the ratio for the electrical spin signal.

To confirm that the large temperature dependence of the spin signal is a common feature for thermal spin injection, we also made a similar measurement by interchanging the current and voltage probes. Here, the thermal spin injection was done from the CoFeAl electrode and the spin accumulation was detected by the Py electrode. In this configuration, we see a clear thermal spin signal because of the large spin-dependent Seebeck coefficient for CoFeAl. Note that the ratio of the thermal spin signal at 25 K to that at 295 K is approximately 3.3, which is comparable to the ratio for the electrical spin signal. These results clearly indicate that the large enhancement of the thermal spin signal at low temperature is a unique property of the Py/Cu interface.

To understand the aforementioned properties more quantitatively, we analytically estimated the electrical and thermal spin polarization for each ferromagnetic alloy. According to the one-dimensional spin-diffusion model [37,38], the electrically and thermally excited spin signals with the transparent interfaces can be calculated as follows:

$$\Delta R_S^{ele} \equiv \frac{\Delta V_{ele}}{I} = \frac{P_I P_D R_I R_D R_{Cu}}{[2R_I R_D + R_{Cu}(R_I + R_D)][\cosh(L/\lambda_{Cu}) + \sinh(L/\lambda_{Cu})] + R_{Cu}^2 \sinh(L/\lambda_{Cu})}, \quad (1)$$

$$\Delta R_S^{th} \equiv \frac{\Delta V_{th}}{I^2} = \frac{P_D R_D R_{Cu} \lambda_I S_S \gamma \rho_I}{[2R_I R_D + R_{Cu}(R_I + R_D)][\cosh(L/\lambda_{Cu}) + \sinh(L/\lambda_{Cu})] + R_{Cu}^2 \sinh(L/\lambda_{Cu})}. \quad (2)$$

Here, P_I and P_D are the bulk spin polarizations for the probes of injector and detector, respectively. R_{FI}, R_{FD}, and R_{Cu} represent the spin resistances for the injector, detector, and Cu, respectively. The spin resistance is defined as $2\rho\lambda/[A(1-P^2)]$, where P, ρ, and λ refer to the bulk spin polarization, resistivity, and spin-diffusion length, respectively. P is zero for a nonmagnet. A is the junction area. λ_{Cu} is the spin-diffusion length of Cu. L is the interval distance between the two ferromagnets. S_S is the spin-dependent Seebeck coefficient of the ferromagnet. Since the thermal spin current is generated by the temperature gradient, we use the finite-element program Comsol Multiphysics to simulate the temperature profile at the interface of the ferromagnetic metal and the nonmagnetic metal. The heat power due to Joule heating is proportional to the current squared, and we can assume that $\Delta T = \gamma\rho I^2$. γ is a constant parameter which mainly depends on the thermal conductivity of the ferromagnet and can be estimated from the numerical calculation based on Comsol.

Note that the difference between Eqs. (1) and (2) are only part of the numerator. This is because the diffusion and detection mechanisms for the nonequilibrium spins are completely the same in both situations. Since ΔR_S^{ele} and ΔR_S^{th} were obtained from experiment, we obtain the following relationship:

$$S_S = \frac{\Delta R_S^{th}}{\Delta R_S^{ele}} \frac{2P}{(1-P^2)A\gamma}. \quad (3)$$

We already know the spin polarizations P both for NiFe and CoFeAl. By evaluating γ from the Comsol simulation, we can easily estimate the spin-dependent Seebeck coefficient S_S. For Py, the obtained S_S is -58.8 μV/K at 25 K, showing a remarkable increase compared with -2.86 μV/K at 295 K.

To seek the reason for the significant increase of S_S, we now estimate the Seebeck coefficients for up and down spins from the following relationships:

$$S_C = \frac{G_\uparrow S_\uparrow + G_\downarrow S_\downarrow}{G_\uparrow + G_\downarrow}, \quad (4)$$

$$S_S = S_\uparrow - S_\downarrow, \quad (5)$$

where S_C is the charge Seebeck coefficient in the open circuit. $G_\uparrow$, $G_\downarrow$ are spin-dependent conductance for up-spin and down-spin electrons.

Figure 4 shows the temperature dependence for the Seebeck coefficients, $S_\uparrow$, $S_\downarrow$, S_C, and S_S. Here, the charge Seebeck coefficient shows a monotonic reduction and approaches zero at low temperature. This is a common feature for metallic materials. On the other hand, S_S shows a monotonic increase with decreasing temperature. In particular, its dependence becomes stronger below 105 K. At this temperature, we find that the sign of $S_\uparrow$ is reversed from negative to positive. So, below this temperature, the electrons for up and down spins move oppositely by introducing the temperature gradient. To see this crossover phenomena more clearly, we also estimate the thermal spin polarization $P_S = S_S/S_C$ for Py as a function of temperature. As can be seen in Fig. 4(b), P_S reaches 9.34 at 25 K. We emphasize that these unique features obtained in Py/Cu/Py and Py/Cu/CFA LSVs originate from the thermal

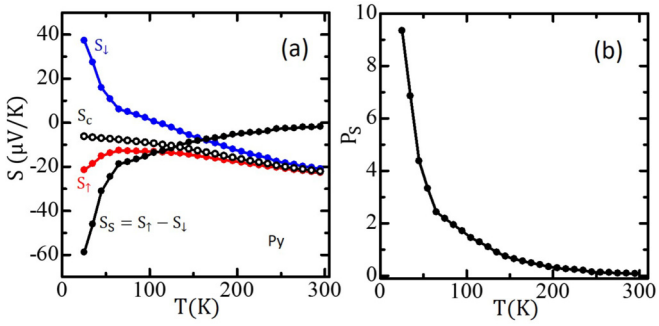

FIG. 4. (a) Seebeck coefficients as a function of temperature from 25 to 295 K. The red and blue circles represent the Seebeck coefficients of up-spin electrons and down-spin electrons, respectively. Open and solid black circles represent the charge Seebeck coefficient (S_C) and and spin-dependent Seebeck coefficient (S_S), respectively. (b) Temperature dependence of thermal-spin-injection efficiency P_S for Py.

TABLE I. Numerically calculated results for the thermo-spin interface parameters at the Py/Cu interface.

m/m_0	$\tilde{G}_\uparrow$ ($\mathrm{m\Omega^{-1}\,\mu m^{-2}}$)	$\tilde{G}_\downarrow$ ($\mathrm{m\Omega^{-1}\,\mu m^{-2}}$)	P	$S_\downarrow/T$ ($\mathrm{nV/K^2}$)	$S_\uparrow/T$ ($\mathrm{nV/K^2}$)	S_S/T ($\mathrm{nV/K^2}$)	$\lvert P_S\rvert$
0.96	1.93	0.84	0.394	-7.5 ± 0.3	27.6 ± 1.2	-35.1 ± 1.2	4.31
0.95	1.90	0.84	0.387	-10.2 ± 0.4	27.6 ± 1.2	-37.8 ± 1.3	11.6
0.91	1.76	0.84	0.354	-2.2 ± 0.3	28.9 ± 1.2	-31.1 ± 1.2	1.40
0.87	1.63	0.82	0.331	1.6 ± 0.4	28.5 ± 1.1	-26.9 ± 1.2	0.80
0.70	1.32	0.81	0.239	9.3 ± 0.3	30.6 ± 0.9	-21.3 ± 1.0	0.34

spin property of Py/Cu interfaces. Thus, even in the Py, the ideal situation for the thermal spin injection can be realized at low temperature.

IV. THEORETICAL CALCULATION

To understand the microscopic reasons for this unique property of the thermal spin injection in the Py/Cu junction, an analysis based on first-principles calculations was executed. According to Mott's law with the Sommerfeld expansion in linear response under the open-circuit condition, the spin-related Seebeck coefficient is expressed as follows [20]:

$$S_\sigma = -eL_0T\partial_E \ln G_\sigma(E)|_{E_F}. \tag{6}$$

Here, σ stands for spin up or spin down, T is the temperature, G_σ is the spin-dependent conductance, $L_0 = \frac{\pi^2}{3}(k_B/e)^2 = 2.45\times10^{-8}\ \mathrm{V^2\,K^{-2}}$ is the Lorenz number with electrical charge e and Boltzmann constant k_B. It should be noted that the magnon contribution is out of consideration in such a simplified calculation [40]. In this sense, all we need is G_σ, which can be calculated by first-principles calculations with the so-called "wave-function-matching" scheme [41–43], as follows:

$$G_\sigma = \frac{e^2}{h}\int dE t_\sigma(E)[-\partial_E f(E,T)], \tag{7}$$

where h is Planck's constant, E is the transport energy, t_σ is the spin-dependent transmission probability, and $f(E,T)$ is the Fermi–Dirac distribution. However, in a ballistic calculation, there will be a contribution to the conductance from the number of channels in the ferromagnetic and nonferromagnetic lead, so the conductance should be corrected by the Schep correction [44,45], which is finally expressed as

$$\frac{1}{\tilde{G}_\sigma} = \frac{h}{e^2}\left[\frac{1}{t_\sigma} - \frac{1}{2}\left(\frac{1}{N_\sigma^{\mathrm{F}}} + \frac{1}{N_\sigma^{\mathrm{N}}}\right)\right], \tag{8}$$

with N_σ^{F} and N_σ^{N} representing the spin-dependent number of channels in the ferromagnetic and nonferromagnetic lead, respectively.

In the realistic calculation, to avoid the disorder-induced scattering in the bulk part of Py, we adapt a Ni/Py/Cu trilayer system with only two-monolayer Py. This is because the calculated spin-dependent Seebeck coefficient is related to the magnetic disorder at the Py/Cu interface. In this model, we set 10×10 supercells, which randomly switch the magnetization direction in the two-monolayer Py. The influence of the temperature is considered as the thermal fluctuation of the magnetization; namely, we assume that the average magnetization could be reduced by increasing the temperature because of the thermal fluctuation. Although the present temperature range is much lower than the Curie temperature of Py, we confirmed that the saturation magnetization of the Py nanowire can be still modified by the thermal fluctuation [46]. This is due to the increase of the surface contributions and is a common feature in patterned nanostructures. In addition, the relatively large magnetic disorder is expected at the Py/Cu interface because of the Ar-ion bombardment [47,48]. Thus, it is a reasonable hypothesis that the scaled magnetization which is the ratio between the average magnetization (m) and the initial magnetization (m_0) represents the temperature.

The calculated results for the spin-dependent conductance $\tilde{G}_\sigma$, $S_\uparrow/T$, $S_\downarrow/T$, $S_S/T = (S_\uparrow - S_\downarrow)/T$ and the thermal spin polarization P_{S} are listed for various scaled magnetization values in Table I. These results indicate that the disorder-induced scattering at the interface strongly affect the spin-dependent parameters. The thermal spin polarization P_{S} shows significant reduction when the value m/m_0 is smaller than 0.95. These calculation results show a good agreement with our experiments. These characteristics have been observed only at the Py/Cu interface and are not observed at the CFA/Cu interface. The relatively low Curie temperature for the Py wire is also related to these unique features.

V. CONCLUSION

In summary, we have systematically studied the temperature dependence of thermal-spin-injection properties for LSVs. A significant enhancement of thermal-spin-injection efficiency was observed only at the Py/Cu interface, resulting in a thermal spin polarization greater than 100% at low temperature. A first-principles calculation including the interface disorder provides the reasonable explanation for this unique temperature dependence. These demonstrations should guide the design of ferromagnetic materials with an efficient thermo-spin conversion effect by using conventional ferromagnets.

ACKNOWLEDGMENTS

This work is partially supported by National Key Research Program of China (Grant No. 2017YFA0206200), National Natural Science Foundation for Young Scholar of China (Grant No. 51601139), China Postdoctoral Science Foundation (Grant No. 2017M613101), Grant-in-Aid for Scientific Research on Innovative Areas, Nano Spin Conversion Science (Grant No. 26103002) and that for Scientific Research (A) (No. 18H03866), and JSPS Program for Fostering Globally Talented Researchers. T.M. acknowledges the support from National Key Research Program of China (Grant No. 2016YFA0300702) and Shanxi Province Science and Technology Innovation Project No. 2015ZS-02.

[1] M. Johnson and R. H. Silsbee, Phys. Rev. B **35**, 4959 (1987).
[2] K. Uchida, S. Takahashi, K. Harii, J. Ieda, W. Koshibae, K. Ando, S. Maekawa, and E. Saitoh, Nature (London) **455**, 778 (2008).
[3] A. Slachter, F. L. Bakker, J.-P. Adam, and B. J. van Wees, Nat. Phys. **6**, 879 (2010).
[4] G. E. W. Bauer, E. Saitoh, and B. J. van Wees, Nat. Mater. **11**, 391 (2012).
[5] L. Gravier, S. Serrano-Guisan, and J.-P. Ansermet, J. Appl. Phys. **97**, 10C501 (2005).
[6] J. Flipse, F. L. Bakker, A. Slachter, F. K. Dejene, and B. J. van Wees, Nat. Nanotechnol. **7**, 166 (2012).
[7] J. Flipse, F. K. Dejene, D. Wagenaar, G. E. W. Bauer, J. Ben Youssef, and B. J. van Wees, Phys. Rev. Lett. **113**, 027601 (2014).
[8] K. Yamasaki, S. Oki, S. Yamada, T. Kanashima, and K. Hamaya, Appl. Phys. Express **8**, 43003 (2015).
[9] H. Yu, S. Granville, D. P. Yu, and J. P. Ansermet, Phys. Rev. Lett. **104**, 146601 (2010).
[10] J. C. Slonczewski, Phys. Rev. B **82**, 054403 (2010).
[11] Z. Yuan, S. Wang, and K. Xia, Solid State Commun. **150**, 548 (2010).
[12] X. Jia, K. Xia, and G. E. W. Bauer, Phys. Rev. Lett. **107**, 176603 (2011).
[13] H. Kohno, Y. Hiraoka, M. Hatami, and G. E. W. Bauer, Phys. Rev. B **94**, 104417 (2016).
[14] G. M. Choi, C. H. Moon, B. C. Min, K. J. Lee, and D. G. Cahill, Nat. Phys. **11**, 576 (2015).
[15] S. Z. Wang and K. Xia, Phys. Rev. B **93**, 184414 (2016).
[16] A. Slachter, F. L. Bakker, and B. J. van Wees, Phys. Rev. B **84**, 020412 (2011).
[17] T. Kikkawa, K. Uchida, Y. Shiomi, Z. Qiu, D. Hou, D. Tian, H. Nakayama, X.-F. Jin, and E. Saitoh, Phys. Rev. Lett. **110**, 067207 (2013).
[18] A. D. Avery, M. R. Pufall, and B. L. Zink, Phys. Rev. Lett. **109**, 196602 (2012).
[19] S. H. Wang, L. K. Zou, J. W. Cai, B. G. Shen, and J. R. Sun, Phys. Rev. B **88**, 214304 (2013).
[20] N. W. Ashcroft and N. D. Mermin, *Solid State Physics* (Saunders, Philadelphia, PA, 1976).
[21] M. Walter, J. Walowski, V. Zbarsky, M. Mzenberg, M. Schers, D. Ebke, G. Reiss, A. Thomas, P. Peretzki, M. Seibt, J. S. Moodera, M. Czerner, M. Bachmann, and C. Heiliger, Nat. Mater. **10**, 742 (2011).
[22] S. Hu, H. Itoh, and T. Kimura, NPG Asia Mater. **6**, e127 (2014).
[23] T. Nomura, T. Ariki, S. Hu, and T. Kimura, J. Phys. D: Appl. Phys. **50**, 465003 (2017).
[24] L. Gravier, A. Fabian, A. Rudolf, A. Cachin, J. E. Wegrowe, and J. P. Ansermet, J. Magn. Magn. Mater. **271**, 153 (2004).
[25] M. Hatami, G. Bauer, Q. Zhang, and P. Kelly, Phys. Rev. Lett. **99**, 066603 (2007).
[26] M. Hatami, G. E. W. Bauer, Q. Zhang, and P. J. Kelly, Phys. Rev. B **79**, 174426 (2009).
[27] Y. Liu, Z. Yuan, R. J. H. Wesselink, A. A. Starikov, M. van Schilfgaarde, and P. J. Kelly, Phys. Rev. B **91**, 220405 (2015).
[28] H. Adachi, K. I. Uchida, E. Saitoh, J. I. Ohe, S. Takahashi, and S. Maekawa, Appl. Phys. Lett. **97**, 2 (2010).
[29] L. J. Cornelissen, J. Shan, and B. J. van Wees, Phys. Rev. B **94**, 180402 (2016).
[30] E. J. Guo, J. Cramer, A. Kehlberger, C. A. Ferguson, D. A. MacLaren, G. Jakob, and M. Kläui, Phys. Rev. X **6**, 031012 (2016).
[31] F. K. Dejene, J. Flipse, and B. van Wees, Phys. Rev. B **86**, 024436 (2012).
[32] T. Kimura, T. Sato, and Y. Otani, Phys. Rev. Lett. **100**, 066602 (2008).
[33] M. Zhu, C. L. Dennis, and R. D. McMichael, Phys. Rev. B **81**, 140407(R) (2010).
[34] E. Villamor, M. Isasa, L. E. Hueso, and F. Casanova, Phys. Rev. B **88**, 184411 (2013).
[35] S. Hu and T. Kimura, Phys. Rev. B **87**, 014424 (2013).
[36] S. Hu, X. Cui, T. Nomura, T. Min, and T. Kimura, Phys. Rev. B **95**, 100403 (2017).
[37] T. Kimura, J. Hamrle, and Y. Otani, Phys. Rev. B **72**, 014461 (2005).
[38] S. Takahashi and S. Maekawa, Phys. Rev. B **67**, 052409 (2003).
[39] L. O'Brien, D. Spivak, J. S. Jeong, K. A. Mkhoyan, P. A. Crowell, and C. Leighton, Phys. Rev. B **93**, 014413 (2016).
[40] R. Iguchi, A. Yagmur, Y.-C. Lau, S. Daimon, E. Saitoh, M. Hayashi, and K. Uchida, Phys. Rev. B **98**, 014402 (2018).
[41] T. Ando, Phys. Rev. B **44**, 8017 (1991).
[42] K. Xia, M. Zwierzycki, M. Talanana, P. J. Kelly, and G. E. W. Bauer, Phys. Rev. B **73**, 064420 (2006).
[43] S. Z. Wang, K. Xia, and G. E. W. Bauer, Phys. Rev. B **90**, 224406 (2014).
[44] K. M. Schep, J. B. A. N. van Hoof, P. J. Kelly, G. E. W. Bauer, and J. E. Inglesfield, Phys. Rev. B **56**, 10805 (1997).
[45] G. E. W. Bauer, K. M. Schep, K. Xia, and P. J. Kelly, J. Phys. D: Appl. Phys. **35**, 2410 (2002).
[46] See Supplemental Material at http://link.aps.org/supplemental/10.1103/PhysRevMaterials.2.104403 for temperature dependence of the saturation magnetization.
[47] C. H. Lai, C. H. Yang, Y. J. Wang, H. Niu, C. Hou, and S. Mao, J. Appl. Phys. **91**, 7101 (2002).
[48] W. Si, K. Williams, M. Campo, M. Mao, A. Devasahayam, and C.-L. Lee, J. Appl. Phys. **97**, 10N901 (2005).